Communication

Automated In Vivo Nano-sensing of Breath-borne Protein Biomarkers

Haoxuan Chen, Jing Li, Xiangyu Zhang, Xinyue Li, Maosheng Yao, and Gengfeng Zheng

Nano Lett., **Just Accepted Manuscript** • DOI: 10.1021/acs.nanolett.8b01070 • Publication Date (Web): 11 Jul 2018

Automated *In Vivo* Nano-sensing of Breath-borne Protein Biomarkers

Haoxuan Chen[1], Jing Li[1], Xiangyu Zhang[1], Xinyue Li[1], Maosheng Yao*[,1] and Gengfeng Zheng*[,2]

[1]State Key Joint Laboratory of Environmental Simulation and Pollution Control, College of Environmental Sciences and Engineering, Peking University, Beijing 100871, China

[2]Laboratory of Advanced Materials, Department of Chemistry and State Key Laboratory of Medical Neurobiology, Fudan University, Shanghai 200438, China

Revision submitted to
Nano Letters

* Corresponding Author:
Maosheng Yao, Email: yao@pku.edu.cn, Ph: +86 01062767282
State Key Joint Laboratory of Environmental Simulation and Pollution Control, College of Environmental Sciences and Engineering, Peking University, Beijing 100871, China

Gengfeng Zheng, Email: gfzheng@fudan.edu.cn
Laboratory of Advanced Materials, Department of Chemistry and Shanghai Key Laboratory of Molecular Catalysis and Innovative Materials, Fudan University, Shanghai 200032, China

June 21, 2018
Beijing, China

Table of Contents Graphic

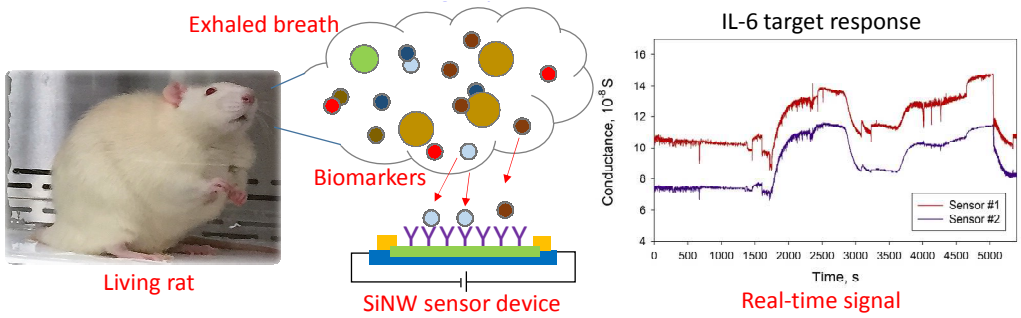

ABSTRACT

Toxicology and bedside medical condition monitoring is often desired to be both ultrasensitive and noninvasive. However, current biomarker analyses for these purposes are mostly offline and fail to detect low marker quantities. Here, we report a system called dLABer (detection of living animal's exhaled breath biomarker) that integrates living rats, breath sampling, microfluidics, and biosensors for the automated tracking of breath-borne biomarkers. Our data show that dLABer could selectively detect (online) and report differences (of up to 10^3-fold) in the levels of inflammation agent interleukin-6 (IL-6) exhaled by rats injected with different ambient particulate matter (PM). The dLABer system was further shown to have an up to 10^4 higher signal-to-noise ratio than that of the enzyme-linked immunosorbent assay (ELISA) when analyzing the same breath samples. In addition, both blood-borne IL-6 levels analyzed via ELISA in rats injected with different PM extracts and PM toxicity determined by a dithiothreitol (DTT) assay agreed well with those determined by the dLABer system. Video recordings further verified that rats exposed to PM with higher toxicity (according to a DTT assay and as revealed by dLABer) appeared to be less physically active. All the data presented here suggest that the dLABer system is capable of real-time, noninvasive monitoring of breath-borne biomarkers with ultrasensitivity. The dLABer system is expected to revolutionize pollutant health effect studies and bedside disease diagnosis as well as physiological condition monitoring at the single-protein level.

Keywords: dLABer, Biomarker, Particulate matter, Toxicity, Biosensor, Real time,

Disease monitoring, Physiological condition

1. Introduction

Epidemiological studies have shown that ambient air pollution is a leading contributor to the global disease burden, *e.g.*, exposure to particulate matter (PM) with a diameter of 2.5 μm ($PM_{2.5}$) is described to have resulted in 4.2 million deaths and 103.1 million disability-adjusted life-years (DALYs) in 2015 (1, 2). For every 10 μg m^{-3} increase in PM_{10}, the respiratory and cardiovascular daily mortality rates were estimated by the World Health Organization (WHO) to be increased by 1.3% (95% CI: 0.5–2.09%) and 0.9% (95% CI: 0.5–1.3%), respectively (3, 4). However, these epidemiological studies strongly rely on the metric of PM mass concentration, while no direct correlation has been established between health outcomes and specific PM components (5-8). Typically, for air pollution health studies, people first collect air samples and store them for some time at low temperature and then conduct the health effect or toxicity studies by exposing the collected air samples to cells or animals (4,5,7-10). PM from different sources could have very different toxicity per unit of mass due to different compositions (9). On the other hand, toxicology studies use cells as subjects, and the results might not apply for humans (10). Although animal-based studies are more representative, biomarker analysis using current methods takes a long time, including taking of blood samples, and importantly, the results might not represent the health state at the time of exposure because biomarker levels evolve over time (11-13). Nonetheless, biomarker analysis is widely used in toxicological studies (14). For example, blood samples from animals are usually taken after

exposure, and then, relevant biomarkers are typically analyzed offline (15, 16). This practice has caused significant problems when interpreting the *in vivo* health effects of environmental pollutants.

Among these health studies, exhaled breath is increasingly being used as a non-invasive biomarker method compared to blood sample for exposure analysis (17-19). Exhaled breath contains a large number of slightly volatile (*e.g.*, nitric oxide, carbon monoxide, hydrocarbons) and nonvolatile compounds (*e.g.*, cytokines, lipids, adenosine, histamine) that can be used to assess the respiratory and systemic health status (20-22). Among the breath-borne substances, fractional exhaled nitric oxide (FeNO), 8-isoprostane, malondialdehyde, interleukins, and other compounds are widely used as markers of oxidative stress and airway inflammation resulting from occupational and daily exposure to air pollutants (23-27). Additionally, exhaled breath has been studied for early diagnosis of lung diseases, such as the use of FeNO for diagnosis and treatment of asthma (28). In many other studies, breath-borne proteins and various cytokines, such as interleukins, TNF-α and leptin, were shown to be associated with lung cancer and can possibly be used for early-stage disease screening (29-31). Technically, breath-borne volatile organic compounds (VOCs) are in the gas phase and can be directly analyzed via gas chromatography-mass spectrometry (GC-MS). Many studies have addressed analysis of breath-borne VOCs from living animal subjects using GC-MS or modified carbon nanotubes (32-34). However, with regard to nonvolatile organic compounds (*e.g.*, proteins, nucleic acids, and viruses), current methods, such as ELISA, for measuring biomarkers take a long time, typically

up to several hours. Recently, the silicon nanowire field effect transistor (SiNW FET) has emerged as a rapid and ultrasensitive tool in the nanoscience field and has already been used to detect many biomolecules, including small molecules, proteins, nucleic acids, viruses, and others (35-40). When detecting biological species, including disease protein biomarkers, the SiNW FET was shown to have a sensitivity up to several orders of magnitude greater than ELISA (41-44). In our previous work, we developed a real-time airborne virus monitoring system (GREATpa) by integrating air sampling, microfluidics and an SiNW sensor device (45). The system has been further successfully applied to detect viruses in exhaled breath condensates with high sensitivity (29 viruses/μl) and selectivity, and the results largely agreed with those from a reverse transcription quantitative polymerase chain reaction (RT-qPCR) analysis (46). Likewise, similar to virus detection, this same system provides an outstanding opportunity for tracking *in situ* PM exposure health effects through real-time monitoring of biomarkers exhaled from animal or human subjects.

Here, we report a new system called dLABer (detection of living animal's exhaled breath biomarker) that integrates living animals, air sampling, and microfluidics as well as a biosensor for the real-time detection of breath-borne biomarkers. The system integrates technologies from various scientific fields, *i.e.*, medical, toxicology, environmental, and nanotechnology fields. To test the system, ambient PM collected from different countries were directly injected into rat blood circulation using a previously reported protocol (47) from our laboratory. IL-6 levels in exposed and control rat breath samples were then monitored in real time using the

dLABer system. The IL-6 levels in collected breath samples were further measured using a standard ELISA for verification and sensitivity comparisons. In addition, IL-6 levels in rat blood sera were also measured. As a confirmation step, the toxicities of PM samples from different cities were also measured using dithiothreitol (DTT). This work develops a frontier method that could potentially revolutionize pollutant health effect studies as well as bedside breath-borne disease diagnosis and monitoring.

2. Materials and methods

2.1 Detection of living animal's exhaled breath biomarker (dLABer) system

In this work, we developed an online PM toxicity analysis system named dLABer, as shown in Figure 1 and Supporting Information S1 (video). The system is composed of three major parts: exhaled breath biomarker collection from living rats, sample delivery, and a biomarker monitoring and analysis module based on a commercial nanobiosensor. For exhaled breath biomarker collection, we constructed a sampler based on the impinging principle that operated at 1 liter breath of air per minute. As observed in Figures 1 and S1, the rat cage was made in-house with only one air inlet (for supplying fresh air to the rats) and one air outlet (for sampling the biomarkers exhaled by the rats). The air was driven by a pump for unidirectional flow in the cage, and biomarkers exhaled by the rats were carried by the air flow and finally absorbed into the collection liquid phosphate-buffered saline (PBS) in a polypropylene conical tube. The conical tube was modified with an outlet in the bottom that allowed the peristaltic pump to automatically transport the sample to the nanobiosensor. The

sample transport flow rate was set to 15 µl per minute and can be adjusted according to experimental need. The initial volume of PBS was 10 ml, and the liquid was automatically replenished by the peristaltic pump at the same speed as sample delivery to maintain a constant volume in the tube during the experiment. For biomarker monitoring and analysis, the commercialized SiNW FET Nanocard (Vista Therapeutics, Inc., USA) was used as the nanobiosensor. Before use, the SiNW was decorated in our laboratory with a rat-specific antibody obtained from an ELISA kit (Becton, Dickinson and Company). When the target antigen bound to the antibody on the nanowire, the conductance of the transistor changed proportionally to the antigen quantity. The detection signal was then programmed using a commercial system (Vista Therapeutics, Inc., USA). Detailed pictures of the biosensor chips used are shown in Figure 2.

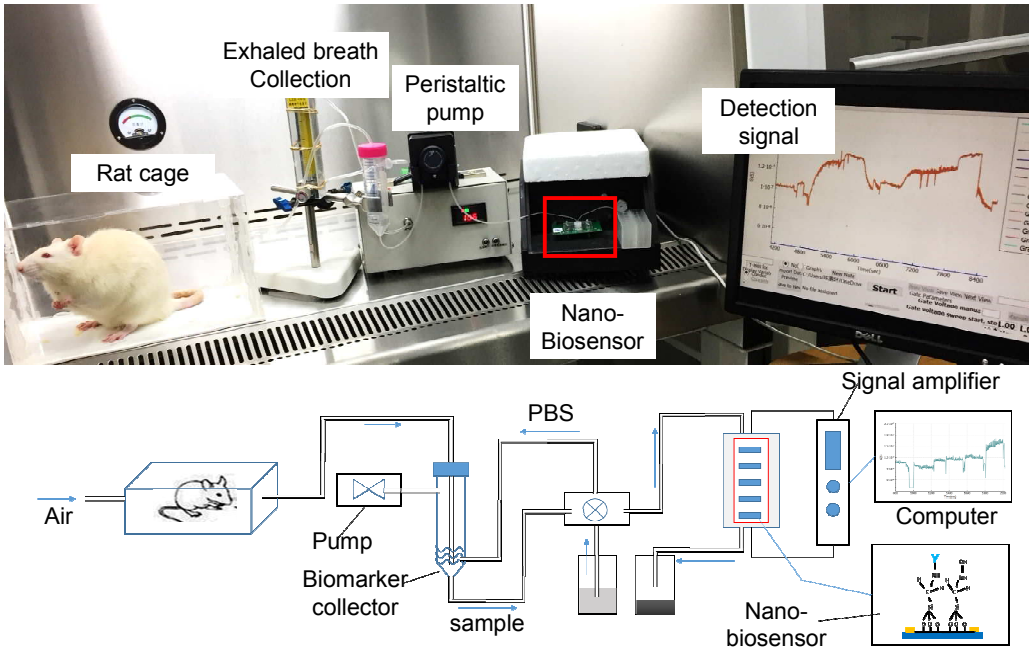

Fig. 1. Experimental sketch and photo of the dLABer system that integrates living rats, breath sampling, microfluidics and a commercial FET-based biosensor for the real-time detection of breath-borne biomarkers; the airborne biomarkers were directly exhaled by the exposed rats (a dLABer system video is provided in Supporting Information S1).

2.2 PM sample collection and suspension preparation

In this work, we applied the dLABer system to real-time analysis of the toxicity of ambient PM collected from different countries by monitoring the IL-6 level in the exhaled breath of rats exposed to the PM via injection. PM samples from different cities (Cities A, B, C and D; these four cities are from four different continents) were collected through automobile air conditioning filters as described in our previous work (48). Detailed analysis of the PM toxicity in the rat model will be reported elsewhere. In this work, the PM samples and the rats were mainly used for testing the dLABer system that was developed. A PM suspension was made by vigorously vortexing 2 mg of dust per ml deionized (DI) water for 20 min at a vortex rate of 3200 rpm (Vortex Genie-2, Scientific Industries Co., Ltd.). The extract solution was then prepared by filtering the PM suspension through a nylon filter with an average pore size of 0.45 μm.

2.3 Rat breeding and PM injection

The jugular vascular catheterization (JVC) rat model described in our previous

work (47) was used to test the dLABer system for the real-time monitoring of breath-borne biomarkers. Thirty male 10-week-old Wistar rats weighing 200–240 g who had undergone a jugular vein catheterization operation were purchased from Beijing Vital River Laboratory Animal Technology Co., Ltd. A flexible sterile catheter was embedded into the jugular vein with approximately 1 centimeter of catheter out of the skin and fixed onto the back of the rat with staples. All the rats were kept in an animal care facility under a natural 12 h light/12 h dark cycle and were fed a normal chow diet. After 1 week of acclimation, the rats were randomly divided into 5 groups (6 rats in each group) for exposure to PM from four different countries or normal saline (NS) as a control. All the groups were injected with the same volume (1 ml) of extract suspension or NS. After injection, one rat from each group was placed in the dLABer system for online exhaled breath biomarker IL-6 analysis, and blood samples were taken (1 ml) 1 hour after injection. The blood serum was separated immediately by centrifugation at 3000 rpm for 4 min, and the serum sample was kept at -20 °C for further analysis. PM extract injection and blood sampling were performed through the embedded catheter using sterile syringes with 23G flat-end needles. All rats were monitored by recording cameras, and the video records were used for analysis of animal behavior in response to different levels of PM exposure. All animal experiments were approved by the Institutional Review Board of Peking University, and relevant experiments were performed in accordance with ethical standards (approval # LA2017204).

2.4 Real-time monitoring of breath-borne biomarkers from PM-injected rats

Before performing experiments, the SiNW sensor (Nanocard) was activated and functionalized in our laboratory by binding an IL-6 antibody to the surface of the nanowires via a two-step procedure described previously (37). First, we used a 1% ethanol/ddH_2O solution containing 10% v:v 3-(trimethoxysilyl)propyl aldehyde to react with SiOH groups for 40 min at room temperature; thereby, aldehyde groups that were used for the next step, i.e., the antibody linkage, were attached to the nanowire surface. The nanowires were washed with isopropanol at 3 µl/min for 20 min and dried under a gentle flow of nitrogen gas for 3-5 min until the entire surface appeared to be dry. Next, the Nanocards were heated overnight (approximately 16 hours) at 40 °C under vacuum. Then, rat IL-6 antibody (Becton, Dickinson and Company) was diluted to 100 µg/ml in 10 mM Na-PBS at pH 8.4 containing 4 mM sodium cyanoborohydride and pulled by a peristaltic pump over the nanowires at 3 µl/min for five hours. Unreacted aldehyde groups on the surface were passivated by reaction with ethanolamine at 6 µl/ml in 10 mM Na-phosphate buffer, pH 8.4, containing 4 mM sodium cyanoborohydride at 3 µl/min for two hours. Finally, Na-phosphate buffer was pulled over the nanowires for 45 min at 3 µl/min. A portable Vista NanoBioSensor unit and NanoBioSensor software (Vista Therapeutics, Inc., USA) were used for conductance signal processing. Recombinant rat IL-6 was serial diluted with PBS and used as a standard. As shown in Figs. 1 and S1, the exhaled breath from the rats was continuously collected using a homemade liquid sampler and transported to the biosensor for real-time breath-borne biomarker analysis.

2.5 Measurements of IL-6 using an enzyme-linked immunosorbent assay

In addition, for quality control, the IL-6 levels in exhaled breath samples and blood samples from the same rats were analyzed using traditional ELISA kits for rat IL-6 detection (Becton, Dickinson and Company) according to the manufacturer's instructions. Briefly, solid-phase IL-6 antibody was prepared by coating microliter plate wells with purified rat IL-6 antibody. IL-6 standards, diluted blood serum or exhaled breath samples, detection antibodies (biotinylated), and horseradish peroxidase (HRP) reagent were added to coated wells step by step to form antibody-antigen-antibody-enzyme complexes. Then, 3,3',5,5'-tetramethylbenzidine (TMB) substrate solution was added after the wells were washed. The TMB substrate turned blue after catalysis by HRP. The reaction was terminated by addition of a sulfuric acid solution, and the suspension finally turned yellow. The color change was measured spectrophotometrically at a wavelength of 450 nm, and the biomarker concentrations in the samples were then determined by comparing the optical density (OD) of the samples to a standard curve. In the ELISA, recombinant rat IL-6 was serially diluted with diluent from the assay kit and used as a standard, and a diluent assay and blood samples collected from rats injected with NS were used as controls. The ELISA results were further compared with those from the dLABer system.

2.6 PM toxicity analysis using a DTT assay

A DTT assay was used to analyze the oxidative potential of PM extract samples

from different cities. Briefly, redox-active compounds catalyze the reduction of oxygen to superoxide by DTT, which is oxidized to disulfide. The remaining thiol is allowed to react with 5,5′-dithiobis-2-nitrobenzoic acid (DTNB), generating mixed disulfides and 5-mercapto-2-nitrobenzoic acid (TNBA), which is then measured based on its absorption at 412 nm. The measured ROS generation potentials are expressed as the normalized index of oxidant generation (NIOG) according to (49). The DTT analysis results for different PM samples were compared with those for breath and blood samples analyzed by the dLABer system and by ELISA. In addition, the water-soluble metal elements in PM extract solutions (*i.e.*, Fe, Cu, Zn, Pb, Ni, V, Cr, Mn, Co, Mo, and Cd) were analyzed via inductively coupled plasma mass spectrometry (ICP-MS, Aurora M90, Bruker, Inc., Billerica, MA, USA). The PM extract samples for ICP-MS analysis were diluted 10:1 with Milli-Q water. To analyze PM toxicity, the bacterial community in PM samples from four cities was investigated by high-throughput sequencing. Briefly, 1.5 ml of each PM suspension was prepared for 16S rDNA bacterial amplicon sequencing using the Illumina Miseq 2×300 bp sequencing platform (Sangon Biotech, Inc., Shanghai, China). Microbial DNA was extracted from bacterial colony samples using an E.Z.N.A. Soil DNA Kit (Omega Bio-tek, Norcross, GA, U.S.) according to the manufacturer's protocol. The V3–V4 region of the bacterial 16S ribosomal RNA genes was amplified by polymerase chain reaction (94 °C for 3 min; followed by 5 cycles at 94 °C for 30 s, 45 °C for 30 s, and 62 °C for 30 s; 20 cycles at 94 °C for 20 s and 55 °C for 20 s; 72 °C for 30 s; and a final extension at 72 °C for 5 min) using the primers 341 F

5′-(CCCTACACGACGCTCTTCCGATCTG(barcode)CCTACGGGNGGCWGCAG)-3′ and 805R 5′-(GACTGGAGTTCCTTGGCACCCGAGAATTCCAGACTACHVGGGTATCTAATCC)-3′. PCRs were performed in a 30 μL mixture containing 15 μL of 2× Taq master mix, 1 μL of each primer (10 μM), and 10-20 ng of template DNA. The second polymerase chain reaction round was carried out in the same 30 μl mixture (95 °C for 3 min; followed by 5 cycles at 94 °C for 20 s and 55 °C for 20 s; 72 °C for 30 s; and a final extension at 72 °C for 5 min). After purification using the Agencourt AMPure XP system (Beckman Instruments, Inc., USA) and quantification using a Qubit2.0 DNA detection kit (Life Technologies, Inc., USA), a mixture of amplicons was used for sequencing on an Illumina platform performed by Sangon Biotech, Inc., Shanghai, China.

3. Statistical analysis

In this study, the SiNW FET conductance level data for all samples were not normally distributed; thus, the differences were analyzed via Kruskal-Wallis one-way analysis. Pairwise multiple comparisons (Dunn's method) were performed to analyze differences between all pairs of samples. In addition, the IL-6 concentrations in the blood sera of rats in different groups were analyzed via ELISA. Despite the occurrence of blood clotting in the catheters, at least 5 blood serum samples were obtained for all groups. Differences between groups were analyzed using an independent sample t-test. Differences between NIOG values of PM from different

cities were analyzed using one-way ANOVA. The dLABer, ELISA and DTT analysis results were compared to further validate the accuracy and reliability of the dLABer system. All statistical tests were performed with the statistical component of SigmaPlot 12.5 software (Systat Software, Inc.), and a p value less than 0.05 indicated a statistically significant difference at a confidence level of 95%.

4. Results and discussion

4.1 Calibration of the dLABer system using IL-6 biomarker standards

Recombinant rat IL-6 was serial diluted 10 times with PBS and used as a standard for evaluating the performance of the nanobiosensor. PBS and standard samples of different concentrations, ranging from 5×10^{0} to 5×10^{4} pg/ml, were delivered continuously and successively via a microfluidic channel to the Nanocard at a flow rate of 20 μl/min, which was controlled by the peristaltic pump. Fifteen SiNW FET circuits on the Nanocard conducted electricity, and the conductivity of the circuits changed in response to the amount of IL-6 attached to the SiNW FET surfaces. The SiNW FET conductance data were monitored and recorded in real time using signal collecting and amplifying equipment (NanoBioSensor and its software). The conductance *vs* time data of two good sensor circuits are shown in Figure 2 (A). When PBS flowed through the Nanocard, the conductance levels of SiNW FET remained at approximately 9.1×10^{-8} S for sensor #1 and 6.5×10^{-8} S for sensor #2. The conductance levels decreased rapidly when the Nanocard was held without liquid flow. The decrease was observed again when the system switched between two standard

samples with different IL-6 concentrations. The conductance levels of SiNW FET increased to 8.4×10^{-8} S for sensor #1 and 6.3×10^{-8} S for sensor #2 when detecting IL-6 standard samples of 5 pg/ml, which was comparable to the levels of PBS. The small difference between the 5 pg/ml IL-6 standard sample and PBS might be caused by the different ionic strengths of the two solutions, because the recombinant rat IL-6 was reconstituted with DI water according to the manufacturer's instructions before being diluted in PBS. The difference between PBS and the standard sample of 5 pg/ml was examined and found to be significant, with a p value < 0.05. As observed in Figure 2 (A), IL-6 concentration levels of 5, 50, 500, 5000, and 50000 pg/ml corresponded to average conductance levels of 8.4, 9.4, 9.7, 10.1, and 12.4×10^{-8} S for sensor 1# and 6.3, 6.8, 7.0, 7.3, and 8.7×10^{-8} S for sensor #2. As observed in Figure 2 (A), a 10-fold increase in IL-6 concentration resulted in an ~3-20% increase in the conductance level. This quantitative relationship could vary with sensor chips due to variations in fabrication and functionalization, and thus, the Nanocard should be calibrated with standards and negative controls before use. The linear regression curves for the calibration results are shown in Figure 2 (B). The regression curves were shown to have reasonable linearity, with R^2 values of 0.8744 and 0.8691 for sensor #1 and sensor #2, respectively, indicating that the dLABer system can be used for quantitative determination. As shown in Figure 2 (B), when the 50000 pg/ml IL-6 standard sample was delivered to the Nanocard, the conductance level increased to a very high level, which was different from the conductance change induced by other standard samples (5-5000 pg/ml). This might be partially due to the excessive ionic

strength of the higher concentration standards. Overall, the calibration results showed that the dLABer system has good linearity with respect to biomarker concentration and the corresponding electrical conductance signal.

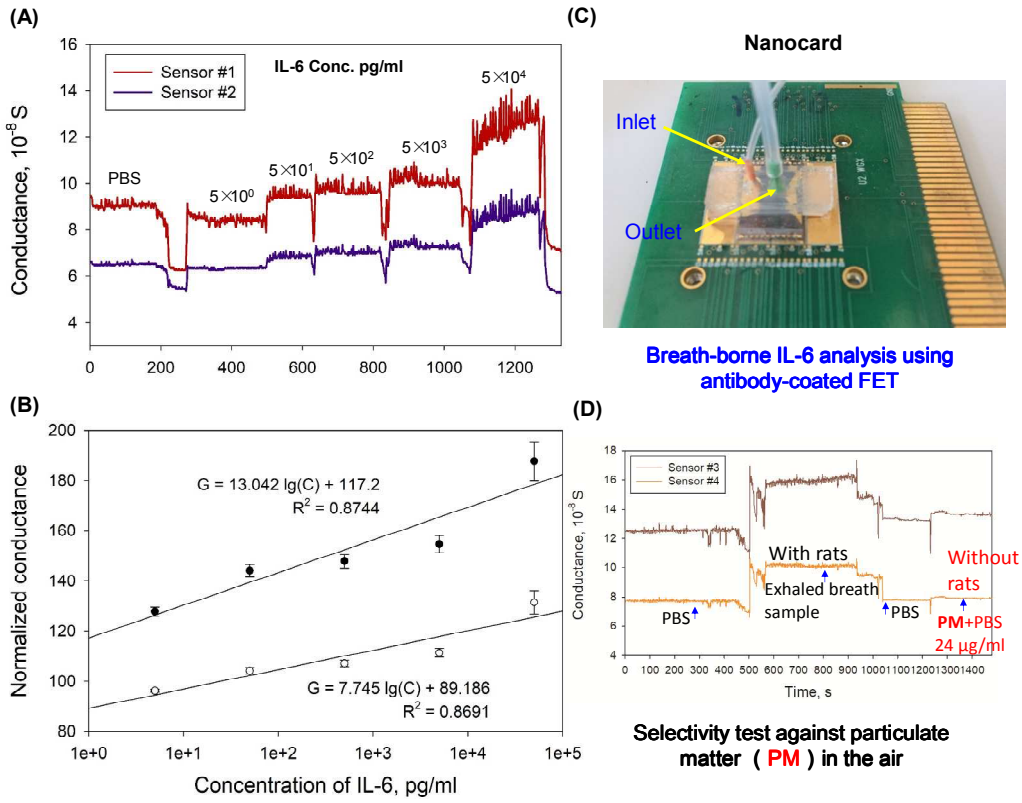

Fig. 2. (A) Detection of rat IL-6 standards using the dLABer system. Two parallel conductance signals from two independent SiNW sensors (Vista Therapeutics, Inc., USA) were selected and are shown in the figure. The corresponding IL-6 concentration (logarithm-transformed) in every standard sample is labeled above the curve in the figure (5×10^0~5×10^4 pg/ml); (B) Linear regression curves of normalized conductance and IL-6 concentration (corresponding to the two conductance curves, drawn from the detection results of rat IL-6 standards); (C) Detailed photos of the commercialized SiNW sensor along with the flow tubes (Vista Therapeutics, Inc., USA); (D) Selectivity test against particulate matter (PM) in the air: detection of IL-6

in exhaled breath samples and PBS buffer solution, which was used to continuously collect PM in the air. An exhaled breath sample was collected from 6 healthy rats inside a cage kept in a lab on the Peking University campus during hazy days for 6 hours. The PM concentration in PBS buffer solution was approximately 24 μg/ml (calculated as follows: 6 h × 6 L/min (air sampling rate) × 110 $\mu g/m^3$ (average ambient PM concentration during the experiments) / 10 ml (volume of PBS buffer)). Two independent SiNW sensor conductance signals are shown in the figure.

As shown in Figure 2 (D), the particulate matter collected from the air did not interfere with nanowire sensing. As shown in this work (described below), the PM in the air also contained many different types of bacteria; and previous studies have also shown that ambient PM contains many different types of viruses (50) and allergens (proteins), such as Der p 1 and Der f 1 (up to 1282 ng/m^3) and endotoxin (up to 83.6 ng/m^3) (51,52). Despite the complex composition of air samples, the conductance signals from the PM, shown in Figure 2 (D), were comparable to those from PBS buffer without the presence of rats. Here, our main application of the technology is on ambient air, thus the non-interferences from the ambient pollutants such as proteins and endotoxin, and microbial particles are very critical. As shown in Figure 2 (A), the sensor responded well to different levels of IL-6. Our ELISA data using the same coating antibody also corresponded well with the dLABer system data (described below). Overall, the system demonstrated outstanding selectivity against many ambient components.

4.2 Detection of IL-6 in exhaled breath samples

After calibration of the nanobiosensor using standards, the dLABer system was used for real-time IL-6 detection in the exhaled breath of rats injected with NS and PM from different cities (A, B, C, and D), as shown in Supporting Information S1. Here, for stable analysis and validation, exhaled breath was first sampled using the dLABer system for 1 hour, and IL-6 in exhaled breath was collected into approximately 10 ml of PBS in collection tubes. After the collection process, the samples were delivered to the nanobiosensor for detection. As shown in Figure 3 (A), a Nanocard was first exposed to PBS, which served as the negative control. The conductance levels were 10.4×10^{-8} S for sensor #1 and 7.3×10^{-8} S for sensor #2, which were higher than the levels observed when PBS was introduced into the Nanocard before calibration. This is largely due to residual attachment of IL-6 from the high-concentration standard sample. Although PBS served as a cleaning solution to detach IL-6 from the SiNW surface, the process required a long time to allow the sensor to return to its original state. Additionally, the affinity between antibody and antigen (IL-6) was an important factor affecting the direction of the reversible reaction. The antibody used has a high K value (chemical equilibrium constant), which indicates easy association and difficult dissociation of antibody and antigen (53). Antibodies with proper affinity could be helpful for improving the reusability of the Nanocard in future applications. A few minutes after the conductance level of PBS became stable, the exhalation samples from rats injected with PM from different cities

were delivered to the Nanocard. As observed in Figure 3 (A), the conductance levels of these samples varied significantly, indicating different IL-6 levels in exhaled breath induced by PM from different cities. The conductance levels were converted into the IL-6 concentration in exhaled breath samples by calculation via the standard curve shown in Figure 2 (B). As shown in Figure 3 (B), rats injected with NS exhibited the lowest IL-6 production. As presented in Figure 3 (B), the signal-to-noise ratios (city PM *vs* NS rat injection) of breath-borne IL-6 measured with the dLABer system ranged from ~10 for City B to ~10^4 for City D.

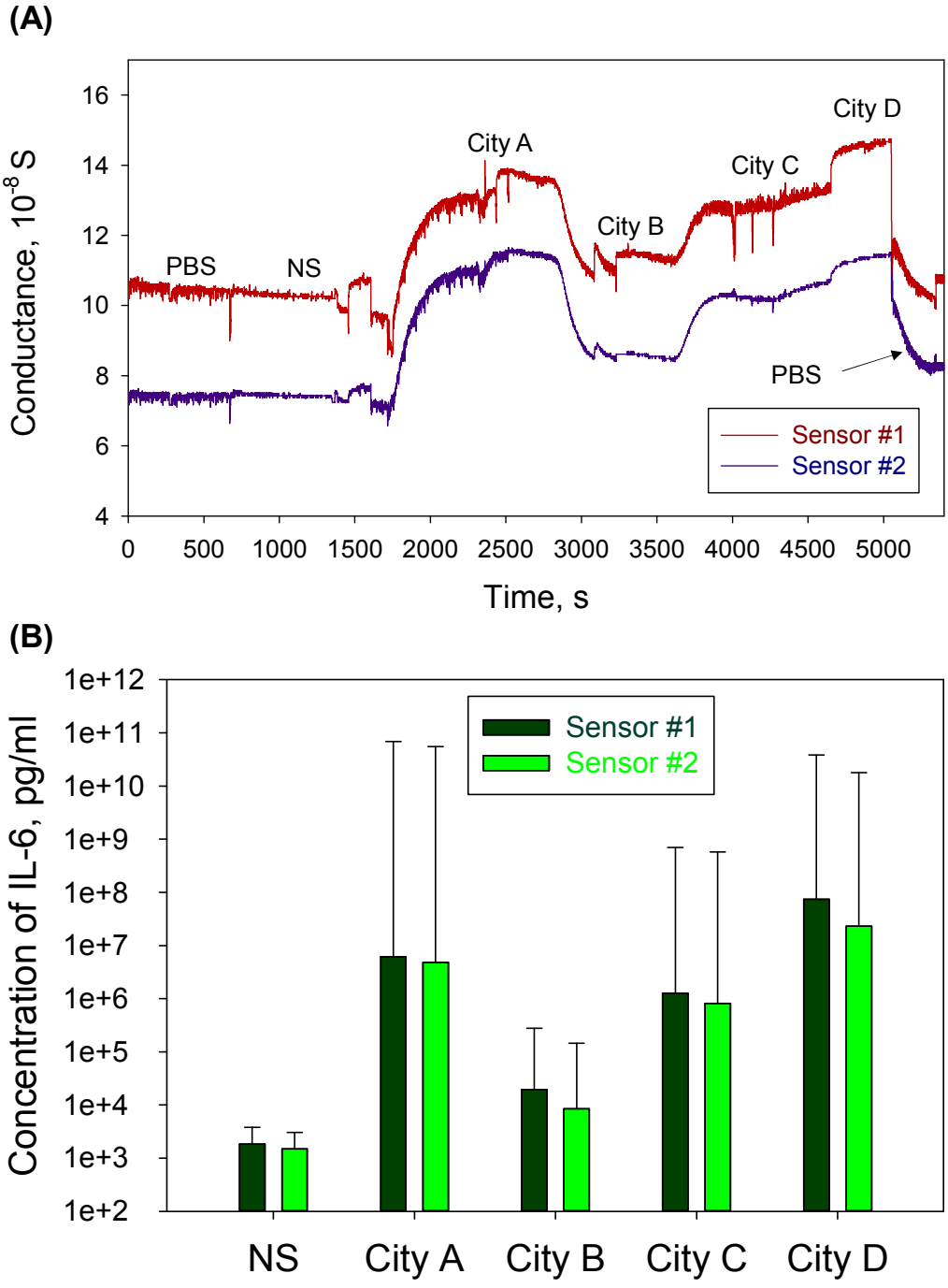

Fig. 3. (A) Detection of IL-6 in exhaled breath samples collected from rats injected with normal saline (NS) and PM from different cities (Cities A-D). The exhaled breath samples were collected 1 h after injection. Two independent SiNW sensor conductance signals are shown in (B); IL-6 concentrations in exhaled breath samples

that correspond to the conductance results are shown in (A) and were calculated using the linear regression curves of IL-6 standards presented in Figure 1.

In our previous *in vivo* study of the toxic effects of PM, the inflammatory marker IL-6 was shown to increase remarkably in serum after injection of PM compared with negative controls injected with NS, indicating that a rapid inflammatory response was induced by PM exposure (47). Other studies have also reported associations between short-term exposure to air pollution and an acute increase in IL-6 (54, 55). As observed in Figure 3 (A), when the exhaled breath sample labeled "City A" flowed into the Nanocard, the conductance level immediately increased to 13 and 11 (x 10^{-8} S) for approximately 7-8 min for sensor #1 and sensor #2, respectively. This conductance fluctuation might be caused by the continuous flow and the fact that there are always some antigens associating with or falling off the antibodies on the SiNW. Rats in each group were injected with the same dose of PM extract (1 ml of 2 mg/ml PM suspension), but the IL-6 levels were different in the exhaled breath of rats in different groups, indicating that different levels of inflammatory responses were induced and the toxicities of PM from different countries are not the same, due to the different components and sources. The PM from City D induced the highest level of IL-6 production in the exhaled breath samples (highest conductance level), followed by Cities A, C, and B. These results, along with those reported in Supporting Information S1, suggest that the dLABer system can detect IL-6 exhaled by rats in real time and thus can distinguish different PM toxicities. The two independent sensors generated

consistent results, and thus, the results showed good repeatability.

Consistent with the above results, as shown in Figure 4 (A) and Supporting Information S2 (videos) taken 1 h after injection, rats exposed to PM from Cities A, C, and D appeared to be drowsy. They remained in the corner of the cage and did not move after the PM injection, while the rats in the NS (control) and City B groups remained relatively active. They moved around the cage and remained alert or curious to external interruptions (*e.g.*, knocking on the cage). Similar behavioral discrepancies were observed between groups of rats injected with high and low doses of PM in our previous study (47), suggesting that the PM injected into the blood circulation system might have caused acute health effects, possibly including nerve injury, in the rats within a short time. The results of this work suggest that the effects of PM from different cities differ due to the PM components and other differences. Overall, the dLABer system can be used for the real-time tracking of breath-borne biomarkers in rats exposed (here, via injection) to PM samples.

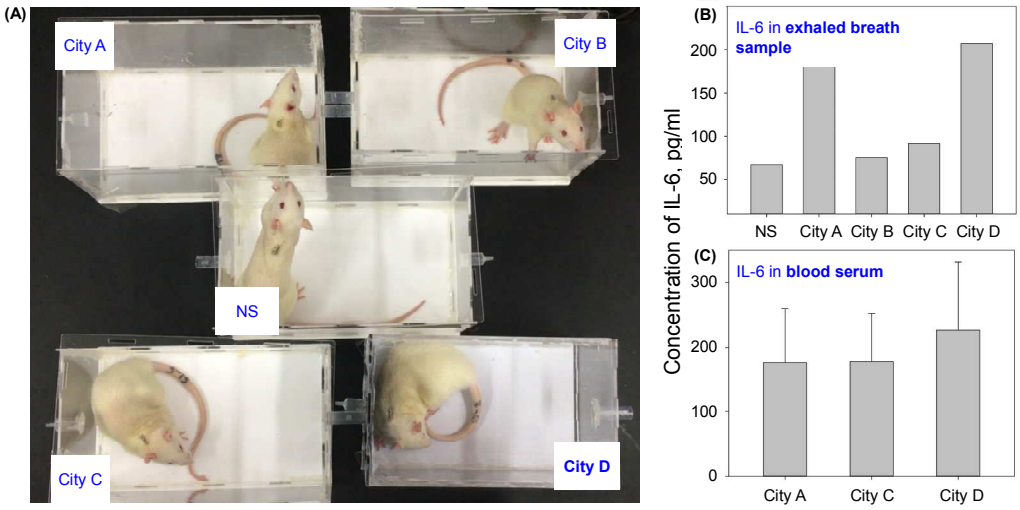

Fig. 4. (A) Video snapshot of rats in groups injected with PM from different cities. Rats in the NS and City B groups appeared to be more active than rats in the City A, C, and D groups, which produced high IL-6 levels in exhaled breath. All related videos are provided in Supporting Information S1. (B) IL-6 levels in the exhaled breath samples from the same rats (analyzed using the dLABer system) assessed with a traditional ELISA ; (C) IL-6 levels in the blood serum of rats injected with normal saline (NS) and PM from different cities measured with a traditional ELISA. The values represent the average concentration of 5 or 6 rats in one group, and error bars indicate standard deviations.

To further validate our method and results obtained using the dLABer system, the IL-6 levels in collected exhaled breath samples (the same samples that were analyzed using dLABer) and blood sera from rats were analyzed via a standard ELISA. As shown in Figure 4 (B), rats injected with PM from City D produced the highest levels of IL-6, followed by Cities A, C, and B. In contrast, rats injected with NS exhibited

the lowest IL-6 levels. These results were consistent with those obtained using the dLABer system. As observed in Figure 3, the dLABer system had a signal-to-noise ratio of 10-10^4, while the ELISA, shown in Figure 4, had a ratio of ~ 1.5-4 when assessing the same breath samples. In addition to the exhaled breath samples, blood samples were taken 1 h after intravenous PM injection, and IL-6 levels were then measured using via ELISA. The average IL-6 levels in the blood samples (after 5-fold dilution) from NS control group and City B group rats were below the detection limit of the ELISA kit; the average IL-6 levels and standard deviations in other groups are shown in Figure 4 (C). As shown in Figure 4 (C), the average IL-6 concentration in blood serum from rats in the City D group was approximately 220 pg/ml, which was higher than that in serum from rats in the City A and City C groups and, unsurprisingly, higher than that in NS and City B group rat sera. In general, these results matched the results obtained with the dLABer system. The PM extracts were intravenously injected through a catheter and induced IL-6 release as a result of systemic inflammation; the IL-6 concentration can increase rapidly in the blood, as revealed in our previous work (47). The results suggested that the IL-6 in blood circulation can be exhaled through pulmonary blood exchange. Upon IL-6 accumulation during sampling, IL-6 can be detected using our dLABer system in real time, as shown in S1. In addition to the real-time breath-borne IL-6 monitoring capability, the dLABer system was found to be more sensitive (up to 10^4 times higher signal-to-noise ratio) than ELISAs when detecting small differences between samples, such the difference between the City B and City C groups. In this work, we collected

airborne IL-6 from a confined space occupied only by rats, as shown in Supporting Information S1 (video); thus, the biomarker would be collected into the liquid even if it came from a different rat-related source. Here, we did not specifically differentiate between potential IL-6 sources, but the IL-6 likely primarily comes from exhaled breath, with a negligible contribution from sweat (56). In theory, the exhaled breath samples were the same temperature as living rats, *i.e.*, 37 °C, but in this work, they were collected into DI water that had a temperature of approximately 20 °C. Accordingly, the temperatures were the same for all breath samples collected and analyzed and the sensors in this work. In the future, experiments could be designed to study the effects of different temperature gradients on sensor responses when analyzing the same breath samples.

Here, the ELISA blood-borne biomarker results agreed with the breath-borne dLABer system results, showing that PM from different cities induced different levels of IL-6 production and thus presented different toxicities. PM is a complex and heterogeneous mixture, and its composition varies greatly with different locations because the emission sources differ (4). Among PM contents, metals are generally studied and have been shown in many studies to cause adverse health effects via ROS generation (57). The metal concentrations in normal saline and PM extracts from different cities in this work are shown in Figure 5 (A). Except for lead (Pb), all metal concentrations in the PM extracts were found to be significantly higher than those in normal saline. Previous studies noted that metals bound to $PM_{2.5}$ could be the

toxicants responsible for ROS generation (induction of oxidative stress) and inflammatory injury (15, 57-59). In addition, one study showed that oxidant radical generation and cytokine production (IL-6 and TNF-α) in airways were significantly increased after administration of metal-rich ambient $PM_{2.5}$ into contralateral lung segments of healthy volunteers (60). The PM from City A and City D had relatively higher Fe, Zn, Mo, and Co levels, while PM from City B had relatively high Mg, Cu, V, and Ni levels. These differences in metal levels might cause different degrees of toxicity, while the contribution of specific elements to toxicity and their possible synergistic mechanisms need to be further investigated. In another study, $PM_{2.5}$ samples collected from a traffic site containing higher concentrations of metals, such as Fe, Cu, Ni, and Mn, *e.g.*, were shown to exhibit higher oxidative ability using a DTT assay (61). The NIOGs of PM from different cities determined by the DTT assay are shown in Figure 5 (B). As observed in the figure, there are significant differences between the NIOGs of the PM from four cities ($p < 0.05$). The PM from City D yielded the highest NIOG, followed by Cities C and A, and the PM from City B exhibited the lowest NIOG. The difference in metal components is shown in Figure 5 (A) and might partially explain the different PM toxicities; however, many chemical and biological materials are present in PM, and their overall contribution to PM toxicity are still not well understood. For example, the biological components, known as bioaerosols, have been found to induce ROS production, and thus, the PM toxicity might be modulated (62). As shown in Figure 5 (C), the bacterial communities in the PM samples collected here varied greatly among the four cities. Among the top 10

bacteria phyla (listed in Supporting Information S3), the proportion of gram-negative bacteria in City A-D samples was 57.15, 54.07, 68.19 and 62.59, respectively. Endotoxins released by these gram-negative bacteria might also contribute to the total toxicity of PM (63, 64).

The NIOG values provided here refer to the ability of the PM to induce oxidative stress and damage, and this index might be a product of numerous factors (65). The proinflammatory behavior of IL-6 in response to toxic compounds and its positive relationship with the level of ROS generation have been well addressed previously (59). Nonetheless, aside from the fact that the PM from City C exhibited a higher NIOG than expected, the DTT assay results for other cities corresponded well with the breath-borne IL-6 results obtained using the dLABer and ELISA methods.

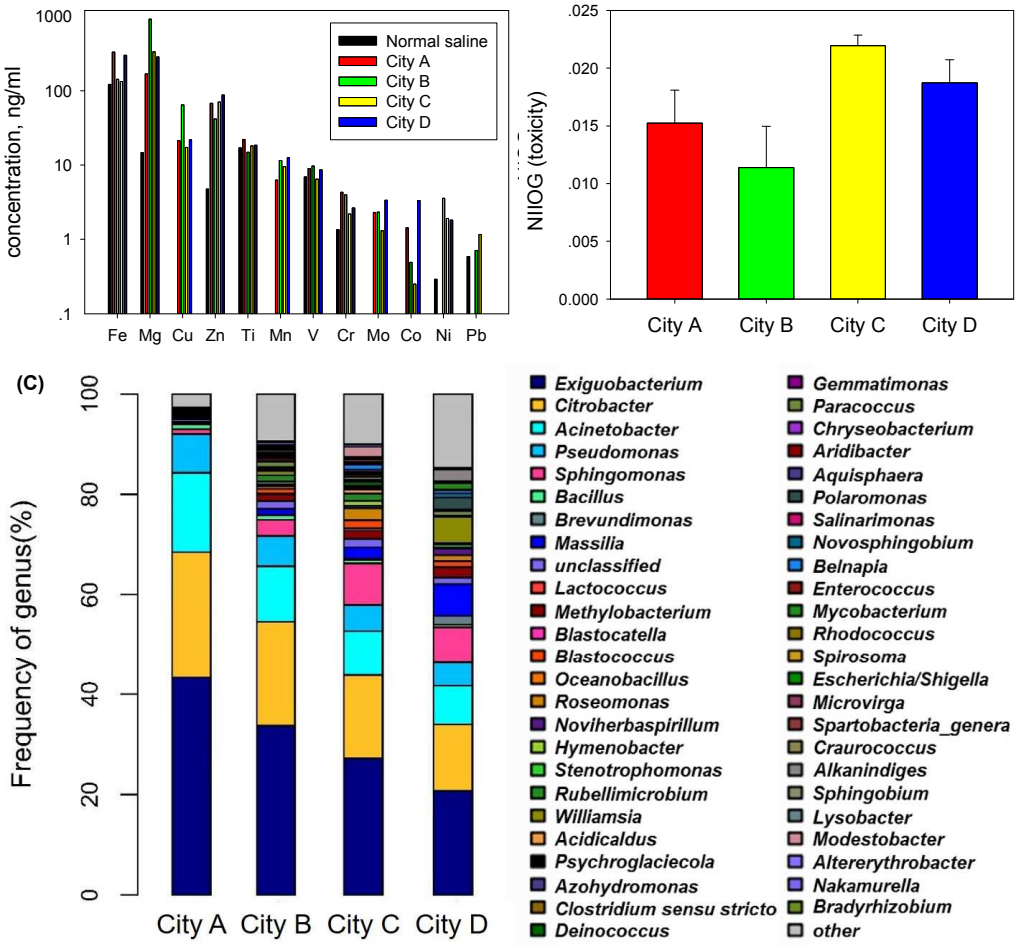

Fig. 5. (A) The measured metal levels in PM suspensions used for injection determined by ICP-MS; (B) Normalized index of oxidant generation (NIOG) determined by the DTT assay for (PM) air samples collected from different cities. The values represent averages of at least 5 samples from each city, and error bars indicate the standard deviation; (C) Culturable bacterial species distribution at the genus level in PM samples from different cities. Different colors in the plot represent different species names corresponding to the text on the right-hand side, and the length of the color block represents the relative abundance of the species. The top 15 bacterial phyla in PM samples from four cities are listed in Supporting Information S3.

Many epidemiological studies have already provided strong evidence that PM pollution is responsible for a variety of diseases, including respiratory disease, cardiovascular illness, and related morbidity and mortality (1). Among these studies, animal model-based toxicology studies have been used to establish cause and effect relationships for specific PM components by precise control of exposure variables. The method typically includes PM exposure (inhalation or tracheal instillation) and subsequent biological analyses, such as biomarker and histopathological analysis. Biomarkers in blood and urine are usually used in both epidemiological and toxicological studies for exposure analysis or pathological analysis. Overall, these studies have led to a good mechanistic understanding of PM health effects. However, the results are often impacted by delayed analysis of *in situ* responses to exposure in human or animal subjects. Biomarkers in living systems are likely to evolve over time; thus, current methods might miss the intermediate health endpoints resulting from pollutant exposure. Compared with other bio-fluids, exhaled breath analysis is noninvasive and more convenient for human subjects Therefore, it has received significant attention in not only environmental health studies but also in other biological and medical studies, such as drug monitoring, pharmacokinetics research (66, 67), and diagnosis of lung disease (21, 68). For example, one study showed that compared with healthy children (IL-4 = 35.7±6.2 pg/ml), children with asthma problems had higher IL-4 levels (53.7±4.2 pg/ml) in exhaled breath condensate, and the IL-4 levels decreased to (37.5±5.6 pg/ml) after steroid treatment (69). In other studies, the IL-6 level increased in the exhaled breath condensate of patients with lung

diseases, such as obstructive sleep apnea (OSA) (70), chronic obstructive pulmonary disease (COPD) (71) and lung cancer (31). Currently, most biomarker analyses, such as those of interleukin in blood, urine, and exhaled breath, are performed through an ELISA. However, ELISAs are time consuming, offline, and not able to track biomarker dynamics in real time. In addition, their sensitivity is relatively low compared with emerging nanotechnology, *e.g.*, field-effect-transistor (FET)-based methods (43). Here, we developed a system called dLABer that integrates living animals, breath sampling, microfluidics, and a FET-biosensor for the real-time monitoring of breath-borne biomarkers. The system is able to overcome both the offline and sensitivity limitations of the current methods. Our results showed that the dLABer system is able to monitor breath-borne IL-6 from rats in real time and provide direct *in situ* evidence of the health effects of PM exposure. Here, the PM exposure level and rats were selected solely to test the developed dLABer system. Undoubtedly, the system could also be used to monitor breath-borne biomarkers exhaled by humans in various scenarios, such as epidemiological studies. Benefiting from its real-time monitoring capability and high sensitivity, the dLABer system can be further developed for evaluation of therapeutic response, pharmacokinetics studies and even bedside monitoring of biomarker-based disease status in the future.

Conclusions

Here, we developed a novel system that allows us to track in real-time breath-borne biomarkers from living subjects. Our work bridges the nanotechnology

field with the environmental, medical and other engineering fields in solving air pollution problems that are often thought to be extremely difficult if not impossible. To test the feasibility of the system, rats injected with PM from different cities were used. The dLABer system results were further validated via ELISA of the breath samples collected. In addition, analysis via ELISA of the blood samples collected from rats injected with different PM samples (of the same mass) and the PM toxicity analysis using the DTT method generally agreed well with the dLABer system results. All the ELISA and DTT assay data and the rat behavior video recordings suggest that the dLABer system is capable of tracking breath-borne biomarkers in real time, with ultrasensitivity, as indicated by the 10^4 higher signal-to-noise ratio than that of the ELISA. Breath-borne biomarkers (proteins), to the best of our knowledge, have not been previously analyzed using nanotechnology, such as SiNW analysis. Thus far, in the air pollution health effect field, no one has taken advantage of the latest cutting-edge nanotechnology for analyzing associated biomarkers, especially for online analysis. Biomarker levels can evolve over time; accordingly, current methods (sample collection and storage for some time, followed by analysis via ELISA or another technique) could miss intermediate health conditions or outcomes due to air pollution exposure. Our work develops an integrated system that can noninvasively monitor the health effects of air pollution in real time or online and, importantly, is able to capture the dynamics of the effect of air pollution on health. Here, rats and PM exposure were selected to test the dLABer system, but in the future, the system could be used along with other types of sensors to detect biomarkers in humans in various

scenarios. The system can be used to immediately monitor breath-borne biomarkers in humans for disease status monitoring or tracking the effectiveness of medications at the bedside. The dLABer system developed here holds great promise for revolutionizing pollutant health effect studies and bedside disease diagnosis, as well as physiological condition monitoring at the single-protein level.

Associated Content

Supporting information

S1. Video of the dLABer system showing real-time breath-borne biomarker monitoring

S2. Video clip of rats 1 hour after injection with PM from different countries

S3. Top 10 bacteria phyla in PM samples from four cities identified using high-throughput sequencing

Acknowledgments

This study was supported by the NSFC Distinguished Young Scholars Fund Awarded to M. Yao (21725701), the National Natural Science Foundation of China (91543126, 21611130103, 21477003, and 41121004), and the Ministry of Science and Technology (2016YFC0207102, 2015CB553401, and 2015DFG92040). A patent has been filed for the dLABer system, and the authors declare no competing interests.

References

1. Cohen AJ*, et al.* (2017) Estimates and 25-year trends of the global burden of disease attributable to ambient air pollution: an analysis of data from the Global Burden of Diseases Study 2015. *The Lancet* 389(10082):1907-1918.

2. Forouzanfar MH*, et al.* (2016) Global, regional, and national comparative risk assessment of 79 behavioural, environmental and occupational, and metabolic risks or clusters of risks, 1990-2013;2015: a systematic analysis for the Global Burden of Disease Study 2015. *The Lancet* 388(10053):1659-1724.

3. WHO (2006) WHO air quality guidelines for particulate matter, ozone, nitrogen dioxide and sulfur dioxide. Global update 2005. Summary of risk assessment. (World Health Organization, http://apps.who.int/iris/bitstream/10665/69477/1/WHO_SDE_PHE_OEH_06.02_eng.pdf).

4. Heal MR, Kumar P, & Harrison RM (2012) Particles, air quality, policy and health. *Chem. Soc. Rev.* 41(19):6606-6630.

5. Kelly FJ & Fussell JC (2012) Size, source and chemical composition as determinants of toxicity attributable to ambient particulate matter. *Atmos. Environ.* 60:504-526.

6. Rückerl R, Schneider A, Breitner S, Cyrys J, & Peters A (2011) Health effects of particulate air pollution: a review of epidemiological evidence. *Inhal. Toxicol.* 23(10):555-592.

7. Cassee FR, Héroux M-E, Gerlofs-Nijland ME, & Kelly FJ (2013) Particulate matter beyond mass: recent health evidence on the role of fractions, chemical constituents and sources of emission. *Inhal. Toxicol.* 25(14):802-812.

8. Lelieveld J & Pöschl U (2017) Chemists can help to solve the air-pollution health crisis. *Nature* 551(7680):291-293.

9. Steenhof M*, et al.* (2011) In vitro toxicity of particulate matter (PM) collected at different sites in the Netherlands is associated with PM composition, size fraction and oxidative potential - the RAPTES project. *Part. Fibre Toxicol.* 8(1):26.

10. Longhin E*, et al.* (2013) Cell cycle alterations induced by urban PM2. 5 in bronchial epithelial cells: characterization of the process and possible mechanisms involved. *Part. Fibre Toxicol.* 10(1):63.

11. Helleday R*, et al.* (2006) Exploring the Time Dependence of Serum Clara Cell Protein as a Biomarker of Pulmonary Injury in Humans. *Chest* 130(3):672-675.

12. Blomberg A*, et al.* (2003) Clara cell protein as a biomarker for ozone-induced lung injury in humans. *Eur. Respir. J.* 22(6):883-888.

13. Pleil JD (2016) Breath biomarkers in toxicology. *Arch. Toxicol.* 90(11):2669-2682.

14. Suhaimi NF & Jalaludin J (2015) Biomarker as a Research Tool in Linking Exposure to Air Particles and Respiratory Health. *BioMed Research International* 2015:10.

15. Pardo M, Shafer MM, Rudich A, Schauer JJ, & Rudich Y (2015) Single Exposure to near Roadway Particulate Matter Leads to Confined Inflammatory and Defense Responses: Possible Role of Metals. *Environ. Sci. Technol.* 49(14):8777-8785.

16. Beck-Speier I, Karg E, Behrendt H, Stoeger T, & Alessandrini F (2012) Ultrafine particles affect the balance of endogenous pro- and anti-inflammatory lipid mediators in the lung: in-vitro and in-vivo studies. *Part. Fibre Toxicol.* 9(1):27.

17. Grob NM, Aytekin M, & Dweik RA (2008) Biomarkers in exhaled breath condensate: a review of collection, processing and analysis. *J. Breath Res.* 2(3):037004.

18. Vereb H, Dietrich AM, Alfeeli B, & Agah M (2011) The Possibilities Will Take Your Breath Away: Breath Analysis for Assessing Environmental Exposure. *Environ. Sci. Technol.* 45(19):8167-8175.

19. Cao W & Duan Y (2006) Breath Analysis: Potential for Clinical Diagnosis and Exposure

Assessment. *Clin. Chem.* 52(5):800-811.

20. Horváth I, Hunt J, & Barnes PJ (2005) Exhaled breath condensate: methodological recommendations and unresolved questions. *Eur. Respir. J.* 26(3):523-548.
21. Horváth I*, et al.* (2017) A european respiratory society technical standard: Exhaled biomarkers in lung disease. *Eur. Respir. J.* 49(4).
22. Kim KH, Jahan SA, & Kabir E (2012) A review of breath analysis for diagnosis of human health. *TrAC Trends in Analytical Chemistry* 33:1-8.
23. De Prins S*, et al.* (2014) Airway oxidative stress and inflammation markers in exhaled breath from children are linked with exposure to black carbon. *Environ. Int.* 73:440-446.
24. Romieu I*, et al.* (2008) Exhaled breath malondialdehyde as a marker of effect of exposure to air pollution in children with asthma. *J. Allergy Clin. Immunol.* 121(4):903-909.e906.
25. Lehtonen H*, et al.* (2007) Increased alveolar nitric oxide concentration and high levels of leukotriene B₄ and 8-isoprostane in exhaled breath condensate in patients with asbestosis. *Thorax* 62(7):602-607.
26. Huang W*, et al.* (2012) Inflammatory and Oxidative Stress Responses of Healthy Young Adults to Changes in Air Quality during the Beijing Olympics. *Am. J. Respir. Crit. Care Med.* 186(11):1150-1159.
27. Pleil JD (2008) Role of Exhaled Breath Biomarkers in Environmental Health Science. *Journal of Toxicology and Environmental Health, Part B* 11(8):613-629.
28. Dweik RA*, et al.* (2011) An Official ATS Clinical Practice Guideline: Interpretation of Exhaled Nitric Oxide Levels (FeNO) for Clinical Applications. *Am. J. Respir. Crit. Care Med.* 184(5):602-615.
29. Chan HP, Lewis C, & Thomas PS (2009) Exhaled breath analysis: Novel approach for early detection of lung cancer. *Lung Cancer* 63(2):164-168.
30. Sarah AH*, et al.* (2016) Exhaled breath condensate for lung cancer protein analysis: a review of methods and biomarkers. *J. Breath Res.* 10(3):034001.
31. Horváth I, Lázár Z, Gyulai N, Kollai M, & Losonczy G (2009) Exhaled biomarkers in lung cancer. *Eur. Respir. J.* 34(1):261-275.
32. Bayn A*, et al.* (2013) Detection of Volatile Organic Compounds in Brucella abortus-Seropositive Bison. *Anal. Chem.* 85(22):11146-11152.
33. Peled N*, et al.* (2012) Detection of volatile organic compounds in cattle naturally infected with Mycobacterium bovis. *Sensors Actuators B: Chem.* 171-172:588-594.
34. Haick H*, et al.* (2009) Sniffing Chronic Renal Failure in Rat Model by an Array of Random Networks of Single-Walled Carbon Nanotubes. *ACS Nano* 3(5):1258-1266.
35. Gao Z*, et al.* (2007) Silicon Nanowire Arrays for Label-Free Detection of DNA. *Anal. Chem.* 79(9):3291-3297.
36. Patolsky F, Zheng G, & Lieber CM (2006) Fabrication of silicon nanowire devices for ultrasensitive, label-free, real-time detection of biological and chemical species. *Nat. Protoc.* 1:1711-1724.
37. Patolsky F*, et al.* (2004) Electrical detection of single viruses. *Proc. Natl. Acad. Sci. U. S. A.* 101(39):14017-14022.
38. Li B-R*, et al.* (2013) An Ultrasensitive Nanowire-Transistor Biosensor for Detecting Dopamine Release from Living PC12 Cells under Hypoxic Stimulation. *J. Am. Chem. Soc.* 135(43):16034-16037.

39. McAlpine MC*, et al.* (2008) Peptide−Nanowire Hybrid Materials for Selective Sensing of Small Molecules. *J. Am. Chem. Soc.* 130(29):9583-9589.

40. Ohno Y, Maehashi K, & Matsumoto K (2010) Label-Free Biosensors Based on Aptamer-Modified Graphene Field-Effect Transistors. *J. Am. Chem. Soc.* 132(51):18012-18013.

41. Cui Y, Wei Q, Park H, & Lieber CM (2001) Nanowire Nanosensors for Highly Sensitive and Selective Detection of Biological and Chemical Species. *Science* 293(5533):1289-1292.

42. Zheng G, Patolsky F, Cui Y, Wang WU, & Lieber CM (2005) Multiplexed electrical detection of cancer markers with nanowire sensor arrays. *Nat. Biotechnol.* 23:1294.

43. Zhang A & Lieber CM (2016) Nano-Bioelectronics. *Chem. Rev.* 116(1):215-257.

44. Stern E*, et al.* (2009) Label-free biomarker detection from whole blood. *Nature Nanotechnology* 5:138.

45. Shen F*, et al.* (2011) Integrating Silicon Nanowire Field Effect Transistor, Microfluidics and Air Sampling Techniques For Real-Time Monitoring Biological Aerosols. *Environ. Sci. Technol.* 45(17):7473-7480.

46. Shen F*, et al.* (2012) Rapid flu diagnosis using silicon nanowire sensor. *Nano Lett.* 12(7):3722-3730.

47. Zhang X, Kang J, Chen H, Yao M, & Wang J (2018) PM2.5 Meets Blood: In vivo Damages and Immune Defense. *Aerosol and Air Quality Research* 18(2):456-470.

48. Li J*, et al.* (2013) Characterization of biological aerosol exposure risks from automobile air conditioning system. *Environ. Sci. Technol.* 47(18):10660.

49. Li Q, Wyatt A, & Kamens RM (2009) Oxidant generation and toxicity enhancement of aged-diesel exhaust. *Atmos. Environ.* 43(5):1037-1042.

50. Cao C, et al (2014) Inhalable microorganisms in beijing's PM2.5 and PM10 pollutants during a severe smog event. *Environ. Sci. Technol* 48:1499-1507.

51. Yao M, et al (2009) A comparison of airborne and dust-borne allergens and toxins collected from home, office and outdoor environments both in New Haven, United States and Nanjing, China. *Aerobiologia* 25:183-192.

52. Yao M, et al (2009) Comparison of Electrostatic Collection and Liquid Impinging Methods when Collecting Airborne House Dust Allergens, Endotoxin and (1,3)-β-D-Glucans. *J Aerosol Sci.* 40: 492-502

53. Braden BC*, et al.* (1995) Protein motion and lock and key complementarity in antigen-antibody reactions. *Pharm. Acta Helv.* 69(4):225-230.

54. Thompson AM*, et al.* (2010) Baseline repeated measures from controlled human exposure studies: associations between ambient air pollution exposure and the systemic inflammatory biomarkers IL-6 and fibrinogen. *Environ. Health Perspect.* 118(1):120-124.

55. Nordenhall C*, et al.* (2000) Airway inflammation following exposure to diesel exhaust: a study of time kinetics using induced sputum. *Eur. Respir. J.* 15(6):1046-1051.

56. Faulkner S, *et al. (2014)* The detection and measurement of interleukin-6 in venous and capillary blood samples, and in sweat collected at rest and during exercise. Eur. J. Appl. Physiol. 114 (6): 1207–1216.

57. Chen LC & Lippmann M (2009) Effects of Metals within Ambient Air Particulate Matter (PM)

on Human Health. *Inhal. Toxicol.* 21(1):1-31.

58. Carter JD, Ghio AJ, Samet JM, & Devlin RB (1997) Cytokine Production by Human Airway Epithelial Cells after Exposure to an Air Pollution Particle Is Metal-Dependent. *Toxicol. Appl. Pharmacol.* 146(2):180-188.
59. Thompson AMS*, et al.* (2010) Baseline repeated measures from controlled human exposure studies: Associations between ambient air pollution exposure and the systemic inflammatory biomarkers IL-6 and fibrinogen. *Environ. Health Perspect.* 118(1):120-124.
60. Schaumann F*, et al.* (2004) Metal-rich Ambient Particles (Particulate Matter2.5) Cause Airway Inflammation in Healthy Subjects. *Am. J. Respir. Crit. Care Med.* 170(8):898-903.
61. Fujitani Y, Furuyama A, Tanabe K, & Hirano S (2017) Comparison of Oxidative Abilities of PM 2.5 Collected at Traffic and Residential Sites in Japan. Contribution of Transition Metals and Primary and Secondary Aerosols. *Aerosol and Air Quality Research* 17(2):574-587.
62. Samake A*, et al.* (2017) The unexpected role of bioaerosols in the Oxidative Potential of PM. *Sci. Rep.* 7(1):10978.
63. Long CM*, et al.* (2001) A pilot investigation of the relative toxicity of indoor and outdoor fine particles: In vitro effects of endotoxin and other particulate properties. *Environ. Health Perspect.* 109(10):1019-1026.
64. Zhang Y, Gaekwad J, Wolfert MA, & Boons G-J (2007) Modulation of Innate Immune Responses with Synthetic Lipid A Derivatives. *J. Am. Chem. Soc.* 129(16):5200-5216.
65. Sameenoi Y*, et al.* (2012) Microfluidic Electrochemical Sensor for On-Line Monitoring of Aerosol Oxidative Activity. *J. Am. Chem. Soc.* 134(25):10562-10568.
66. Li X*, et al.* (2015) Drug Pharmacokinetics Determined by Real-Time Analysis of Mouse Breath. *Angewandte Chemie International Edition* 54(27):7815-7818.
67. Khoubnasabjafari M, Rahimpour E, & Jouyban A (2018) Exhaled breath condensate as an alternative sample for drug monitoring. *Bioanalysis* 10(2):61-64.
68. Hunt J (2002) Exhaled breath condensate: An evolving tool for noninvasive evaluation of lung disease. *J. Allergy Clin. Immunol.* 110(1):28-34.
69. Shahid SK, Kharitonov SA, Wilson NM, Bush A, & Barnes PJ (2002) Increased Interleukin-4 and Decreased Interferon-γ in Exhaled Breath Condensate of Children with Asthma. *Am. J. Respir. Crit. Care Med.* 165(9):1290-1293.
70. Carpagnano GE*, et al.* (2002) Increased 8-Isoprostane and Interleukin-6 in Breath Condensate of Obstructive Sleep Apnea Patients. *Chest* 122(4):1162-1167.
71. Bucchioni E, Kharitonov SA, Allegra L, & Barnes PJ (2003) High levels of interleukin-6 in the exhaled breath condensate of patients with COPD. *Respir. Med.* 97(12):1299-1302.